A Study of TCSC Controller Design for Power System Stability Improvement

Alberto D. Del Rosso, *Member, IEEE*, Claudio A. Cañizares, *Senior Member, IEEE*, and Victor M. Doña

***Abstract*—Different control aspects related to the use of TCSC for stability improvement of power systems are addressed in this paper. A novel hierarchical control designed for both dynamic and steady state stability enhancement is proposed, and a complete analysis is presented of various locally measurable input signals that can be used for the controller. Control strategies to mitigate adverse interactions among the TCSC hierarchical controls are also presented. A simplified model of the Argentinean high voltage interconnected system is used to illustrate the ideas presented in the paper.**

***Index Terms*—Stability enhancement, FACTS, TCSC, controller design, hierarchical control.**

I. Introduction

THE potential benefits of using Flexible AC Transmission system (FACTS) controllers for enhancing power system stability are well known. The use of these controllers give grid planners and operators a greater flexibility regarding the type of control actions that can be taken at any given time. Thyristor Controlled Series Capacitors (TCSC), in particular, have been widely studied and reported in the technical literature, and have been shown and used in practice to significantly enhance system stability [1], [2].

In dynamic applications of TCSCs, various control techniques and designs have been proposed for damping power oscillations to improve system dynamic response, whereas for steady state control, the main interest of users and researchers has been the use of the this controller for power flow control in transmission lines, usually considering optimal scheduling strategies (e.g. [3], [4]). Most of the available technical literature in TCSC usually deals with steady state and dynamic control and applications independently. However, to fully understand and properly utilize these types of controllers, a number of control tasks for both dynamic and steady state system improvement must be jointly considered [2]. Since the time frames of the different control actions comprise a wide range of system responses, a hierarchical control scheme should be preferably considered for the controller. In the case of a TCSC, such a scheme should consider the different control levels acting on the same control variable, which in this paper is assumed to be the fundamental frequency equivalent impedance, as this is the control variable most commonly studied in the literature. In this kind of hierarchical control design, adverse interactions between the different control levels may be expected when not properly coordinated [4], [5].

The main aim of this paper is to analyze the design of a hierarchical TCSC controller for stability enhancement, taking into account interactions among the different control levels. A linear dynamic compensator with various input signals for damping power oscillations is proposed and studied based on a typical stability model of the TCSC. Since large-disturbance stability improvement is of major concern here, tuning of the control parameters is mainly carried out via simulations of severe fault conditions. Two different control strategies to mitigate adverse effects of the TCSC steady state set point are proposed, based on the controller performance under major disturbances, and considering that the set point value may be defined by an "upper" control level designed for power flow rescheduling. The performance of the proposed controls is illustrated using an 89-bus, 72-machine model of the Argentinean power grid.

The paper is structured as follows: Section II briefly describes the control scheme of a typical TCSC controller, as well as the controller model used in this paper. The design of the proposed TCSC hierarchical control loops and the selection of adequate input signals are thoroughly discussed in Section III. In Section IV, the test system model based on the Argentinean power grid is described, together with a brief description of the analysis and simulation tools used in this work; the results of applying the proposed TCSC controller design for stability enhancement of the test system are also discussed in this section. Finally, Section V summarizes the main contributions of this paper.

II. TCSC Modeling and Basic Control Scheme

A typical TCSC module consists of a fixed series capacitor (FC) in parallel with a thyristor controlled reactor (TCR). The TCR is formed by a reactor in series with a bi-directional thyristor valve that is fired with a phase angle α ranging between 90º and 180º with respect to the capacitor voltage [2].

Submitted to *IEEE Trans. Power Systems* September 2002; revised and resubmitted January 2003; accepted for publication February 2003.

This work was partially supported by the National Science and Engineering Research Council (NSERC) of Canada.

A. D. Del Rosso is with Mercados Energeticos, Estudios Eléctricos, L.N. Alem 584, Pisos 11 y 13 (1001), Buenos Aires, Argentina (e-mail: adelrosso@mercadosenergeticos.com.ar).

C. A. Cañizares is with the Dept. of Electrical & Computer Engineering, University of Waterloo, Waterloo, ON, N2L-3G1, Canada (e-mail: c.canizares@ece.uwaterloo.ca).

V. M. Doña is with the Instituto de Energía Eléctrica (IEE), Universidad Nacional de San Juan, San Juan, Argentina (email: vdona@iee.unsj.edu.ar).

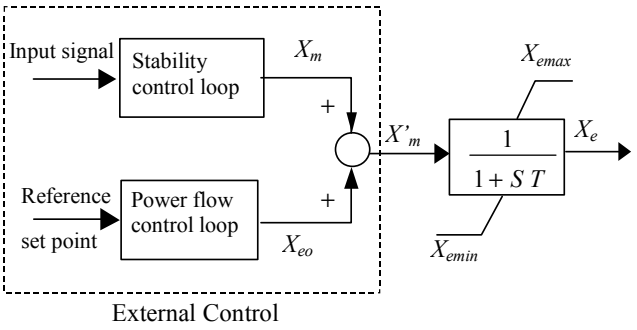

Fig. 1. TCSC model for stability studies.

In a TCSC, two main operational blocks can be clearly identified, i.e. an external control and an internal control [6]. The function of the external control is to operate the controller to accomplish specified compensation objectives; this control directly relies on measured systems variables to define the reference for the internal control, which is usually the value of the controller reactance. The function of the internal control is to provide appropriate gate drive signals for the thyristor valve to produce the desired compensating reactance. Thus, the external control is the one that defines the functional operation of the controller [3], [6].

The external control may be comprised of different control loops depending on the control objectives. Typically, the principal steady state function of a TCSC is power flow control, which is usually accomplished either automatically with a "slow" PI controller or manually through direct operator intervention. Additional functions for stability improvement, such as damping controls, may be included in the external control [4], [5], [7].

The general block diagram of the TCSC model and external control structure used in this work is shown in Fig. 1. In this figure, X_m is the stability control modulation reactance value, as determined by the stability or dynamic control loop, and X_{eo} denotes the TCSC steady state reactance or set point, whose value is provided by the power flow or steady state control loop. The sum of these two values yields X'_m, which is the final value of the reactance ordered by the external control block. This signal is put through a first-order lag to represent the natural response of the device and the delay introduced by the internal control, which yields the equivalent capacitive reactance X_e of the TCSC [8] (in this paper, $X_e > 0$). This model is valid for dynamic and steady state stability analyses, i.e. for balanced, fundamental frequency system conditions.

In [9], a TCSC model suitable for voltage and angle stability applications and power flows studies is discussed. In that model, the equivalent impedance X_e of the device is represented as a function of the firing angle α, based on the assumption of a sinusoidal steady-state controller current. In this model, it is possible to directly represent some of the actual TCSC internal control blocks associated with the firing angle control, as opposed to just modeling them with a first-order lag function. Nevertheless, since the relationship between angle α and the equivalent fundamental frequency impedance X_e is a unique-valued function [9], the TCSC is modeled here as a variable capacitive reactance within the operating region defined by the limits imposed by the firing angle α. Thus, $X_{emin} \le X_e \le X_{emax}$, with $X_{emax} = X_e(\alpha_{min})$ and $X_{emin} = X_e(180^o) = X_C$, where X_C is the reactance of the TCSC capacitor. (In this paper, the controller is assumed to operate only in the capacitive region, i.e. $\alpha_{min} > \alpha_r$, where α_r corresponds to the resonant point, as the inductive region associated with $90^o < \alpha < \alpha_r$ induces high harmonics that cannot be properly modeled in stability studies [6].)

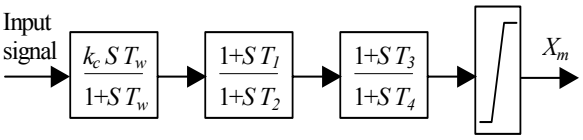

Fig. 2. Transfer function of the proposed stability control loop.

III. External Control Design

If the power flow control loop is "slow", as is typically the case for a PI controller with a large time constant or for manual control, X_{eo} is assumed here to be constant during large-disturbance transient periods. In the particular case of a PI power flow control, a protection logic scheme may be implemented to avoid contradictory control signals that could degrade the overall controller performance [4]; thus, in this paper, the power flow control is assumed to be disabled after large disturbances, keeping X_{eo} at a fixed value during severe transients.

When the system is subjected to a severe disturbance, the stability control loop must provide maximum compensation level during the immediate post-fault period, so that the synchronizing torque is increased to improve the first-swing stability response of the system, as well as provide proper modulation to damp the subsequent power oscillations. In this paper, a linear controller is proposed for stability enhancement, since, with a proper selection of control parameters and input signals, this control can meet the aforementioned control requirements.

The general structure of the proposed stability controller is depicted in Fig. 2. It consists of a washout filter, a dynamic compensator, and a limiter. The washout filter is needed to avoid a controller response to the dc offset of the input signal. The dynamic compensator consists of two (or more) lead-lag blocks to provide the necessary phase-lead characteristics. Finally, the limiter is used to improve controller response to large deviations in the input signal.

Two fundamental elements in this controller design process, i.e. input signal and parameter tuning, are discussed below. The effect of set point value on controller performance, and particularly its effect on interactions between the stability control loop (dynamic control) and the power flow control

loop (steady state control), is also discussed.

A. Input Signals

The selection of the appropriate input signal is a fundamental issue in the design of an effective and robust controller. The following are some of the main characteristics of a proper input signal:

- The input signal should preferably be locally measurable. This is desirable to avoid additional costs associated with communication and to improve reliability.
- The oscillation modes to be damped should be "observable'" in the input signal. Mode observability analysis can be used to select the most effective signal to damp out the critical modes under consideration.
- The selected input signal must yield correct control actions when a severe fault occurs in the system.

Line active power, line reactive power, line current magnitude and bus voltage magnitudes are all candidates to be considered in the selection of input signals for the TCSC stability control loop. Of these possible input signals, active power and current are the most commonly discussed in the literature. Thus, in [5], the authors point out that there is not a big difference in damping performance when either the active power or line current is used as input signals; however, this conclusion was reached based only on small disturbance analyses using linearized models of the power system. In [10], on the other hand, it is shown that when active power is used as an input signal of a controller that introduces a large phase lead, the control signal may lead to negative damping problems in the case of severe system disturbances with large changes in generator power angles. Hence, in this paper, both line active power and current magnitudes are considered and compared as candidate input signals for the stability controller.

A qualitative analysis of the performance of the TCSC stability control loop for both line power flow P and line current magnitude I input signals, can be carried out on the simple single machine-infinite bus (SMIB) test system depicted in Fig. 3, following some of the analysis techniques proposed in [10] and applying the equal area criterion. Thus, assuming in the SMIB system that a solid three-phase fault is applied and then cleared at the generator terminals, the pre-fault and post-fault equivalent impedance are the same. If the classical machine model is used and the resistance on the network is neglected, the generator real power can be expressed as

$$P = \frac{E' V_s}{X - X_e} \sin(\delta) \qquad (1)$$

where X is the equivalent reactance of the transmission link without the compensator (including the reactance of the transformer and the line as well as the generator's transient reactance), E' is the constant transient emf of the generator, and δ is the internal generator phase angle.

Neglecting the TCSC's first order lag associated with the natural response of the controller in Fig. 2, the TCSC equivalent impedance is given by $X_e = X_{eo} + X_m$. Thus, the

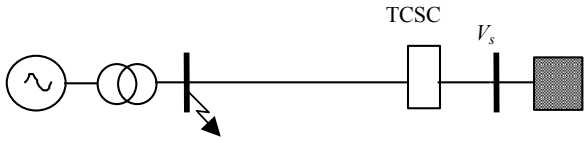

Fig. 3. Single machine-infinite bus system example.

magnitude of the line current is defined as

$$I = \frac{1}{X - X_e} \sqrt{E'^2 + V_s^2 - 2 E' V_s \cos(\delta)} \qquad (2)$$

For simplicity, it is assumed here that the stability control is comprised of a pure derivative block and a constant gain k_c. Hence, denoting the input signal as y (representing either P or I), the controlled reactance may be defined as

$$X_m(t) = k_c \frac{dy(t)}{dt} \qquad (3)$$

If the sensitivity of y with respect to the net transmission reactance (X - X_e) is neglected in both equations (1) and (2), the time derivative of the input signal y can be expressed as follows (observe that E' and V_s are both assumed constant):

$$\frac{dy(t)}{dt} = \frac{\partial y}{\partial \delta} \frac{d\delta}{dt} = \frac{\partial y}{\partial \delta} \Delta\omega \qquad (4)$$

Thus, for any given speed deviation $\Delta\omega$, the value of the control reactance X_m, i.e. control output, is determined by the value of the partial derivative $\partial y/\partial \delta$. When line active power P is the input signal, $\partial P/\partial \delta$ is the largest at δ = 0 and decreases as δ approaches 90°, becoming zero at δ = 90° and turning negative for $\delta > 90°$. This indicates that for δ values near 90°, when the control should provide the largest possible compensation, since P is at its maximum value, X_m is practically zero and hence ineffective; furthermore, for $\delta > 90°$ the control signal changes sign causing undesirable negative damping effects [10]. Notice that at any typical operating point with $\delta << 90°$, a small disturbance will produce a correct control signal and positive damping.

The zero output and negative damping problem is not an issue when the line current magnitude I is used as the input, as the control output signal has the correct sign over the whole range of power angle variation, as it can be observed from the behavior of $\partial I/\partial \delta$ resulting from (2) [10].

These issues can be further clarified by using the equal area criterion. Thus, Figs. 4 and 5 depict the power-angle curves for the SMIB system when the line current magnitude I and power P are the input signals, respectively. In Fig. 4, curve B represent the pre-fault system P-δ curves, whereas curves A and C illustrate the trajectories the system follows during the forward swing and the backward swing ($\Delta\omega < 0$), respectively, for X_m defined by (3). Point 1 is the initial operating point and area 1-2-3-4 represents the energy released during the fault-on period, as the fault is assumed to be cleared at point 3.

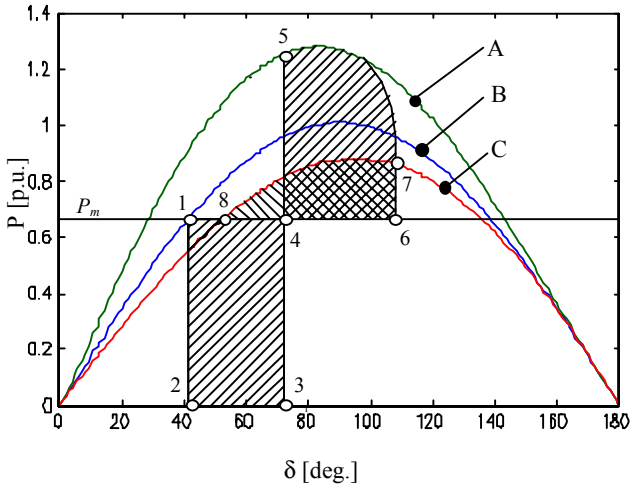

Fig. 4. Equal Area criterion for line current magnitude as input signal.

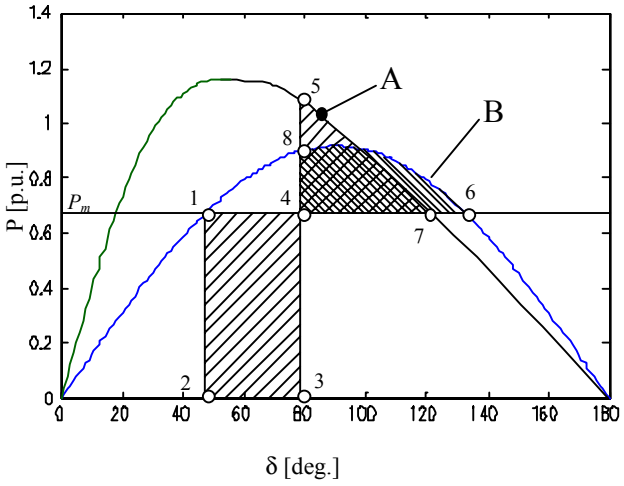

Fig. 5. Equal Area criterion for active power flow as input signal.

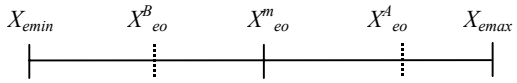

Fig. 6. Set point variations.

Due to the stability control loop, the TCSC capacitive reactance is increased at the instant of fault clearance resulting in the system tracing curve A. At point 6, the speed deviation becomes zero, as the decelerating area 4-5-7-6 equals the accelerating area, and thus the rotor commences its backward swing. During this back swing, the stability control decreases the TCSC reactance value and hence the system traces curve C. Observe that the deceleration area defined by curve A is greater than the deceleration area that would be obtained without TCSC control action, which is basically the area defined by curve B. Furthermore, the accelerating area 4-6-7-8 in the backward swing is smaller than the corresponding one obtained without TCSC reactance modulation. The same process continues in the subsequent oscillations, thus significantly improving oscillation damping in this case.

For the case of input signal P depicted in Fig. 5, B is the pre-fault system P-δ curve, as in the case of input signal I. Curve A is the trajectory the system follows during the forward swing when the control reactance X_m is defined by (3). Observe that the deceleration area 4-8-5-7 is slightly less than the corresponding area 4-8-6-7 defined by curve B, which represents the deceleration area when there is no TCSC stability control in the system, and hence significantly smaller than the deceleration area obtained in the case of input signal I. Thus, the control action when the active power is used as the input signal is much less effective. Furthermore, for operating states with high power transfer levels it may degrade instead of improve system dynamic performance, as the swinging angle may easily exceed 90^o and hence result in negative damping, as previously explained; this is not the case at low level power transfer levels, where the stability control would lead typically to correct control action, given that $\delta(t) < 90^o \ \forall$ t.

This qualitative analysis for both line power and current as input signals is confirmed by the simulation results obtained for the realistic test system discussed in Section IV.

Although this paper concentrates on comparing the use of P and I as input signals for the TCSC stability control loop, as previously discussed, it is important to highlight the fact that the line reactive power Q may also be used as an effective input signal, given that its behavior with respect to δ is similar to the one shown by the line current I. Thus, following a similar argument as the one used to analyze P and I, it can be readily shown that $\partial Q/\partial\delta$ is a sine curve, which results on the reactive power having a correct sign in the whole range of power angle variations; furthermore, in the vicinity of $\delta = 0$, when the control is less effective, the signal is small, increasing with the angle and reaching its maximum at $\delta = \pi/2$, where the control is the most effective.

B. Parameter Tuning

A number of alternative techniques may be used for selection of TCSC control parameters. The most popular ones, which are based on linear systems theory, are phase and gain margin techniques, pole placement through root locus analysis, eigenvalue placement based on residues, and optimal selection of control parameters based on eigenvalues sensitivities (e.g. [11], [12], [13]). However, the TCSC damping effect and associated control parameters behave highly nonlinearly [14]; hence, linear techniques can only guarantee adequate controller operation locally, i.e. the controller operates properly around the limited number of operating points used for its parameter tuning (this is particularly true for those controllers tuned based on eigenvalue sensitivity calculations). Thus, when the major concern is the controller's performance under severe disturbances, which typically trigger large excursions of generator angles, power flows, bus voltages, and other system variables due to the nonlinear characteristics of the power system, analyses based on system linearizations or small signal approximations do not usually provide adequate results, as demonstrated in [14] as well as Section IV for a realistic test system. An initial controller design may be

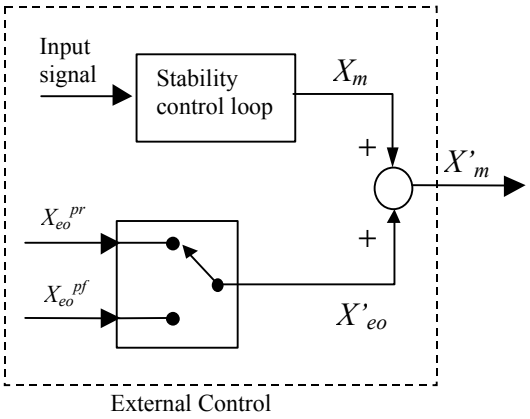

Fig. 7. Pre-fault and post-fault TCSC set point strategy.

carried out using any of the aforementioned linear techniques, but the control parameters should then be adjusted using full time-domain simulations that incorporate all system nonlinearities and limit settings, as well as consider multiple realistic large-disturbance scenarios.

C. Hierarchical Control Design

For the TCSC external control structure defined in Section II (Fig. 1), the power flow control loop action defines the value of X_{eo} within the allowable operating range depicted in Fig. 6. When a severe disturbance is produced, first, the stability control loop significantly increases the TCSC equivalent reactance X_e to reduce the amplitude of the first swing, and then its value oscillates around the reference set point $X_{ref} = X_{eo}$. If X_{eo} is close to the upper limit, the TCSC output saturates at X_{emax}, resulting in a poorly damped system. On the other hand, if X_{eo} is near the lower limit, the controller may be too "slow" and, as a consequence, the TCSC reactance may not be high enough to control the first swing after the fault, resulting in loss of synchronism [7]. In other words, for a given fault, the system may be stable and properly damped for $X_{eo} = X^m_{eo}$ in Fig. 6, but lightly damped for $X_{eo} = X^A_{eo,}$ or just unstable for $X_{eo} = X^B_{eo}$, as demonstrated by the simulation results discussed in Section IV for a realistic test system.

From the previous discussion, it is clear that it is not feasible to tune the control parameters so that the system response is robust for any value of the TCSC reactance set point; an optimal tuning for a given set point may not be adequate for other values of X_{eo}. Observe that a limiter in the power flow control channel can be used, with tighter limits on X_{eo} than the limits on the TCSC control output depicted in Fig. 1, so that enough reactance margin for stability control modulation can be ensured when X_{eo} is at its limits. However, this would not fully resolve the problem of improperly damped oscillations. Thus, two different control strategies to avoid negative effects of set point values over stability control performance are proposed here.

1) Variable controller gain A variable gain strategy can be developed so that the controller gain k_c changes as the TCSC set point values vary. In this case, the gain k_c and the remaining stability control parameter are set for a certain set point value, say $X_{eo} = X^m_{eo}$, taking into account various operating and fault conditions. This gain is then adjusted on-line for changes in X_{eo}, reducing it when $X_{eo} > X^m_{eo}$ and increasing it for $X_{eo} < X^m_{eo}$. This control strategy can be readily implemented by means of digital controls [4].

Simulations on a test system for different operating and fault conditions showed that by varying k_c in inverse proportion to changes in the set point X_{eo}, the sensitivity of the TCSC controls with respect to changes in X_{eo} is significantly reduced, as demonstrated in Section IV.

2) Variable Post-contingency Set Point Value By implementing the proper control logic, X_{eo} may be set to two independent values associated with the pre-fault (X_{eo}^{pr}) and post-fault (X_{eo}^{pf}) system conditions, as illustrated in Fig. 7.

The procedure to select the values and switch between the pre- and post-fault set points is as follows: When a severe disturbance is detected, the pre-fault TCSC set point X_{eo}^{pr} is automatically switched to the selected post-fault set point X_{eo}^{pf}, so that the damping control modulation reactance X_m oscillates around the post-fault set point value. The value of X_{eo}^{pf} is chosen "far" from the TCSC controller limits to avoid saturation. As previously discussed, it is quite difficult to obtain a control parameter tuning that is robust for any TCSC set-point value; hence, control parameters are tuned for the chosen X_{eo}^{pf} value for different operating and fault conditions, so that proper performance of the stability control is assured.

The advantage of this method over the aforementioned adaptive control technique is its simplicity, as in this case the user has to only pre-select a unique value X_{eo}^{pf}, which is a simpler task than choosing the "correct" on-line strategy to vary the controller gain k_c.

IV. Results

The Power System Toolbox (PST) was used here for all time-domain simulations, eigenvalue calculations and mode observability analyses [15]. This is a MATLAB-based power system analysis toolbox developed to analyze power systems using user-defined models. It has several graphical tools; namely, a voltage stability tool, a transient stability tool, and a small signal stability tool. The models for TCSC and other controllers and devices are included into the toolbox by means of user-defined "modules". The original program code was modified to be able to use different input signals for the existent TCSC controller model.

The simulations results presented here were obtained for a model of the Argentinean high voltage interconnected system (SADI) depicted in Fig. 8. The main characteristics of this system are:

- Transmission lines are long and unmeshed (observe in Fig. 8 the radial nature of this system).
- Main low cost generation areas are far from the major load centers.
- The power transfer capability of interface tie lines is basically defined by stability limits rather than thermal limits.

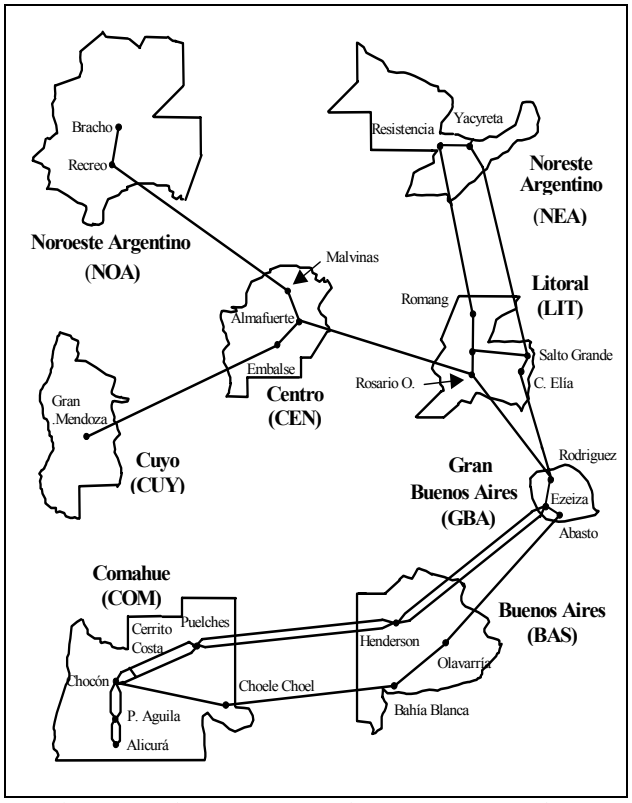

Fig. 8. Argentinean Interconnected System or SADI (500kV).

The principal generation areas are the Comahue (COM) and the Noroeste Argentino (NEA) areas. In these areas, the generation is composed mainly of hydro power plants plus some thermal generation units using low-cost natural gas. The main load centers are located in the Gran Buenos Aires (GBA) and the Buenos Aires (BAS) areas. Two transmission corridors of about 1100 km transmit power from NEA and COM to GBA.

The simplified model of the network used in this paper represents all of the SADI 500 kV buses plus some of its 220 kV buses. The test system consists of 89 nodes, 133 lines and transformers, and 72 equivalent machines. The generators are modeled using a typical transient model for the synchronous machines, exciters, voltage regulators, power systems stabilizers and governors. Loads are represented as constant PQ loads, as these types of loads stress the system more, from the stability point of view, than the typical impedance load models.

The main transmission corridor COM-GBA is studied here, and is primarily composed of a double-circuit line, referred here to as Line A, that goes through Cerrito Costa, Puelches, Henderson and Ezeiza, and a single-circuit line, referred here to as Line B, that goes through Chocón-Choele, Choel, Bahia Blanca, Olavarría and Abasto. This corridor is currently comprised of series-compensated lines with fixed capacitor banks at a compensation level of about 50%. The limits on the maximum active power that the corridor is able to transmit are basically imposed by stability issues.

TABLE I
EIGENVALUES AND MODE OBSERVABILITY

Line out	Mode	Damping ratio	Frequency [Hz]	*I* Obs.	*P* Obs.
None	1	0.070	0.606	0.824	0.855
	2	0.046	0.711	0.861	0.877
Line B	1	0.011	0.480	0.823	0.298
	2	0.080	0.680	0.809	0.279

For the purposes of this paper, the following TCSC is assumed to be installed at the mid-point of Line A:

- The capacitor fundamental frequency reactance at 50 Hz is $X_C = 39\ \Omega$.
- The TCSC ratio $r_C = X_C/X_L$ is assumed to be $r_C = 10$ (X_L is the fundamental frequency impedance of the TCR), which yields a resonant point at $\alpha_r = 150^o$.
- The firing angle limits are hence assumed to be $\alpha_{max} = 180^o$ and $\alpha_{min} = 155^o$, which correspond to limits in the TCSC equivalent capacitive reactance of $X_{emin} = 39\ \Omega$ and $X_{emax} = 96.4\ \Omega$.
- The TCSC steady-state capacitive reactance or set point adopted for simulations is $X_{eo} = 58\ \Omega$ ($\alpha_o = 158.6^o$), which corresponds to a compensation level of 44 %.

Different operating conditions are considered, corresponding to various power levels transmitted through the COM-GBA corridor associated with different power generation dispatch settings in the COM area. The total load of the system is assumed to be $P_L = 11404$ MW and $Q_L = 4800$ MVAR, and is kept unchanged for all study cases. The total generated power for the base-case conditions is $P_G = 11820$ MW and $Q_G = 4170$ MVAR, yielding power flows through Line A and Line B of $P_A = 1742$ MW and $P_B = 822$ MW, respectively. Only one severe contingency corresponding to a three-phase fault on Line B near the Chocón bus, followed by a tripping of the line, is considered.

A. Input Signals

The active power *P* and the current magnitude *I* through the line where the TCSC is located are considered here as possible input signals. As discussed in Section II, an appropriate feedback signal should have significant observability of the critical modes that need to be damped out. Hence, mode observability analyses, as described in [11], are carried out for these two signals considering different operating conditions associated with the pre-contingency and post-contingency networks.

Table I shows the results of the open loop eigenvalue and mode observability analysis for an operating condition where the power generated in the COM area is increased with respect to the base-case; thus, the power flows on Line A and Line B in this case are $P_A = 1948$ MW and $P_B = 907$ MW, respectively (an 219 MW increment in the total power transferred with respect to the base-case). The system presents two poorly damped electromechanical modes; mode shape analysis in the pre-contingency network shows that these

TABLE II
PARAMETERS OF THE TCSC CONTROLLER

k_c	T_w	T_1	T_2	T_3	T_4
1.1	5	1.1	0.05	0.08	0.5

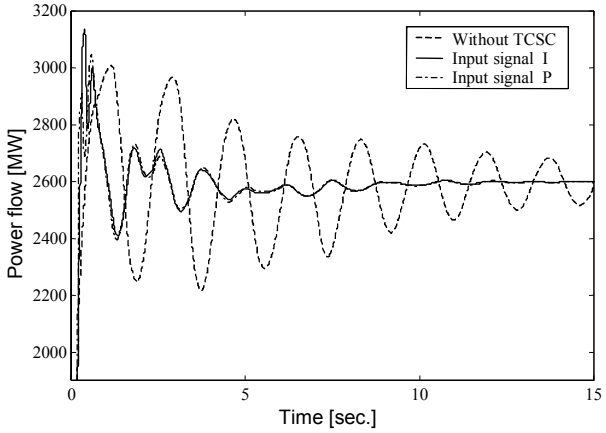

Fig. 9. Power flow variations on Line A, Case 1.

correspond to inter-area modes. In the pre-fault state, the observability indices of the two modes for the *P* and *I* signals are very similar and close to 1 (the maximum possible value). However, in the post-fault state, i.e. with Line B out, the observability of the modes in *I* is considerably greater than in *P*. Therefore, one would expect that the performance of the TCSC controller when using line current as the input signal would be better than when the active power is used, especially for the stressed system when a critical transmission line is tripped off as a consequence of a fault. Time-domain simulations confirm these results, as discussed below.

B. Parameter Tuning

The parameter values for the TCSC model used in this paper are given in Table II. These values correspond to the best-tuned controller for the test system, and were initially obtained using a pole placement linear technique for the base-case operating conditions, to then retune them based on multiple time-domain simulations with the aim of improving the transient response of the system for the contingency under study at various operating conditions.

C. Stability Improvements

1) Case 1 The operating conditions considered in this case correspond to the base-case generation in the COM area. The aforementioned fault is applied at t = 0.1 s, and cleared after 100 ms.

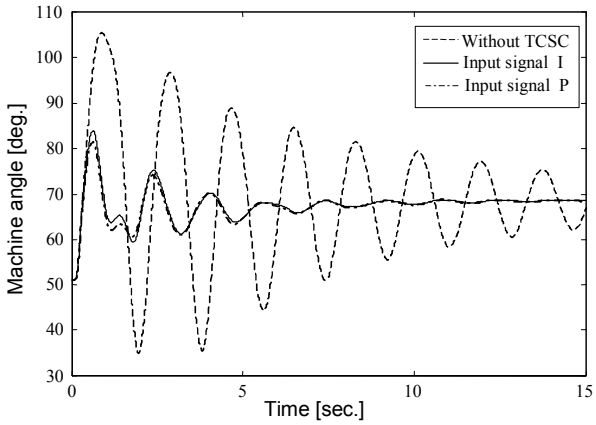

Fig. 10. Machine angle variations, Case 1.

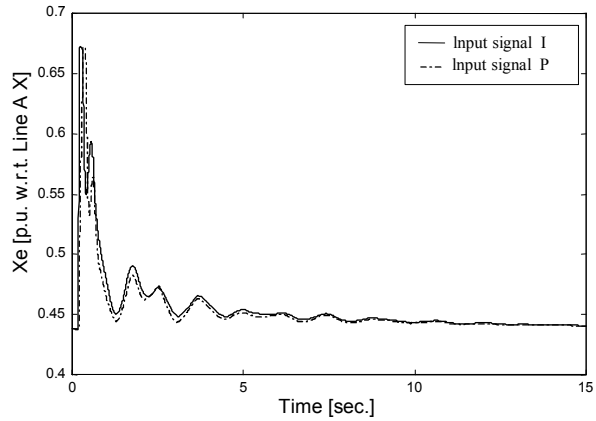

Fig. 11. TCSC equivalent reactance variations, Case 1.

Figure 9 illustrates the time response of the active power flow in Line A, i.e. the line where the TCSC is installed, for three different system conditions; namely, for the system without TCSC, and for the system with the TCSC controller for both current and active power control input signals. The results clearly show that the system without TCSC is first-swing stable for this fault, but post-contingency oscillations are not well damped. The TCSC controller significantly reduces the first rotor angle swing and improves the damping of the subsequent power swings, for both input signals, as expected from the observability analysis.

Figure 10 depicts the internal angle oscillations with respect to the reference generator of the machine that is most severely affected by the fault, whereas Fig. 11 illustrates the variations of the TCSC fundamental frequency reactance.

2) Case 2 The generation in the COM area is increased so that the power flows on Line A and Line B are P_A =2100 MW and P_B =958 MW, respectively (a 494 MW increment on the total transmitted power with respect to the base-case). The same contingency is simulated in this case.

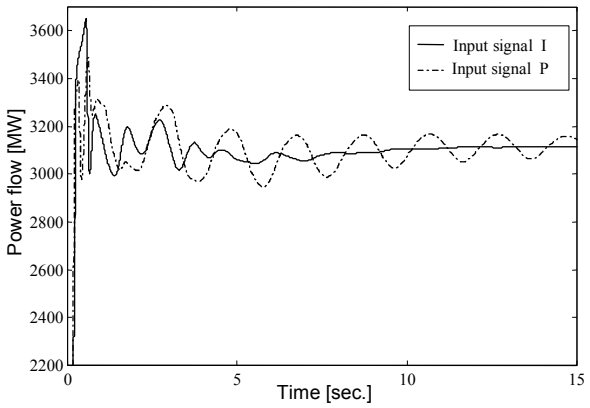

Fig. 12. Power flow variations on Line A, Case 2.

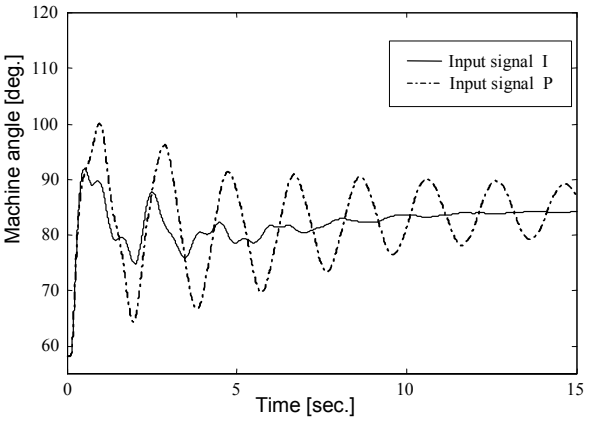

Fig. 13. Machine angle variations, Case 2.

In Figs. 12 and 13, the Line A power flow and machine angle excursions for the most severely affected machine are depicted for the two TCSC control input signals; without the TCSC, the systems is transiently unstable, losing synchronism in the first swing (not shown in these figures). The TCSC stabilizes the system and damps the remaining oscillations with both input signals; however, observe that the performance of the controller when *I* is used as the input signal is much better than when *P* is utilized. This confirms the results obtained from the mode observability analysis, as well as the analyses presented in Section III.

D. Set Point Variations

To illustrate the effect of varying the TCSC set point on the dynamic system response of the system, the COM area generation is set so that the total power transmitted through the COM-GBA corridor is 2885 MW (a 321 MW increment with respect to the base-case), and the same contingency as in the previous cases is applied. The three cases illustrated in Table III are studied; these differ from each other only in the value of the TCSC set point for the pre-fault system. The current magnitude *I* is used as the controller input signal in all cases.

TABLE III
TEST CASES

Case	X_{eo} [Ω]	Comp. [%]	P_A [MW]	P_B [MW]
A	58	44	1970	915
B	79	60	2092	793
C	46	35	1908	977

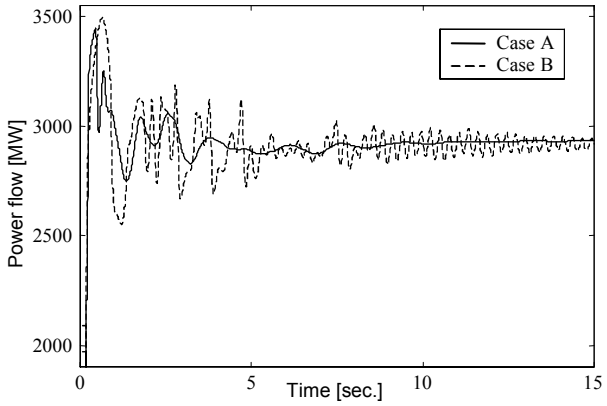

Fig. 14. Power flow variations on Line A, set point studies.

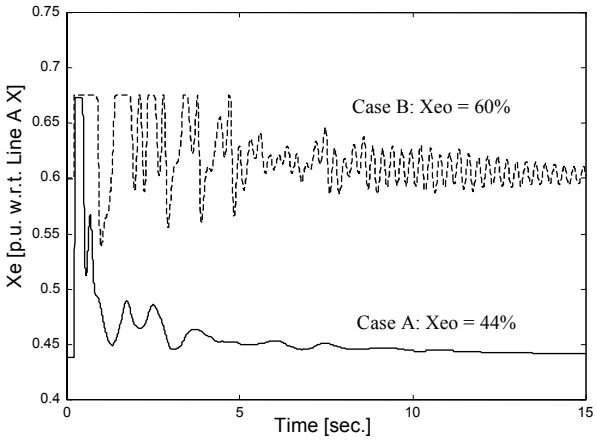

Fig. 15. TCSC equivalent reactance variations, set point studies.

Case C is unstable, as the system loses synchronism in the first swing, and hence is not depicted in Figs. 14 and 15; this illustrates the discussion in Section III regarding low set point values that do not yield enough damping to stabilize the system after a large disturbance. The effect of controller saturation corresponding to a set point value close to the upper reactance limit (Case B) can be clearly observed in these figures, as the power oscillations are not well damped when compared to a "proper" set point value (Case A). It is important to point out that the TCSC control parameters have been optimally tuned for Case A (X_{eo} = 58 Ω); hence, large deviations from this value affect controller performance, resulting in a degraded system dynamic response.

The results of varying the controller gain and the post-contingency set point for these three study cases are discussed and illustrated below.

TABLE IV
CONTROLLER GAIN VARIATIONS

Case	X_{eo} [Ω]	Comp. [%]	k_c
A	58	44	1.1
B1	79	60	0.7
C1	46	35	1.4

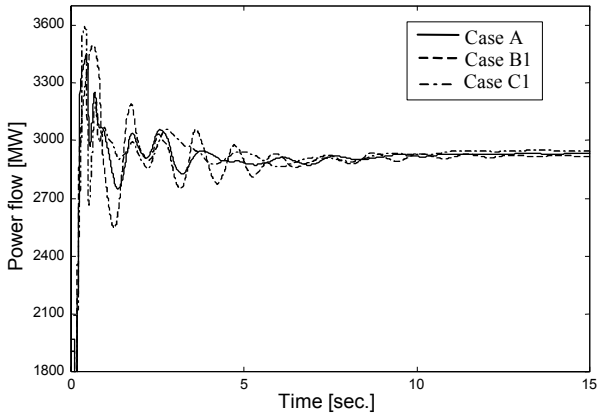

Fig. 16. Power flow variations on Line A, variable controller gain.

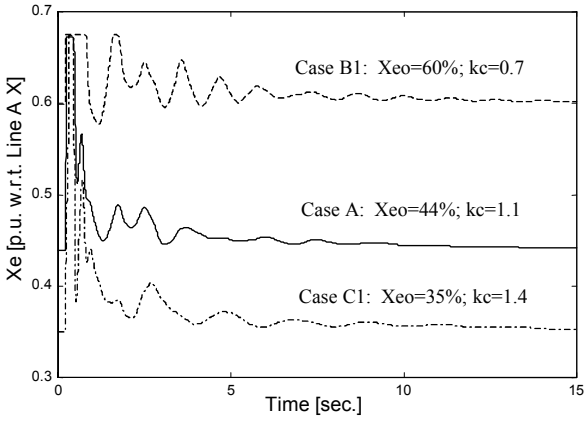

Fig. 17. TCSC equivalent reactance variations, variable controller gain.

1) Variable Controller Gain As discussed in Section III, by "adapting" the value of the controller gain k_c to TCSC set point variations, the system dynamic response can be significantly improved. Table IV shows the optimal k_c values for each of the test cases in Table III; Figs. 16 and 17 depict the simulation results corresponding to Figs. 14 and 15. Observe that this control strategy leads to satisfactory controller performance for all of the X_{eo} values considered.

2) Variable Post-contingency Set Point Value The value adopted for the post-contingency TCSC reactance set point X_{eo}^{pf} for all the three cases illustrated in Table V is 58 Ω (44 % compensation level); the TCSC control parameter values are tuned to this set point value, i.e. k_c = 1.1. Figures 18 and 19 illustrate the results of applying this control strategy, showing an improvement in controller performance.

TABLE V
CONTROLLER SET POINT VARIATIONS

Case	X_{eo}^{pr} [Ω (%)]	X_{eo}^{pf} [Ω (%)]	k_c
A	58 (44)	58 (44)	1.1
B2	79 (60)	58 (44)	1.1
C2	46 (35)	58 (44)	1.1

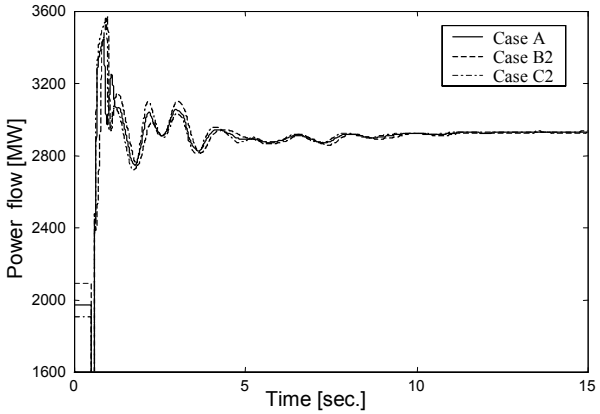

Fig. 18. Power flow variations on Line A, variable post-contingency set point.

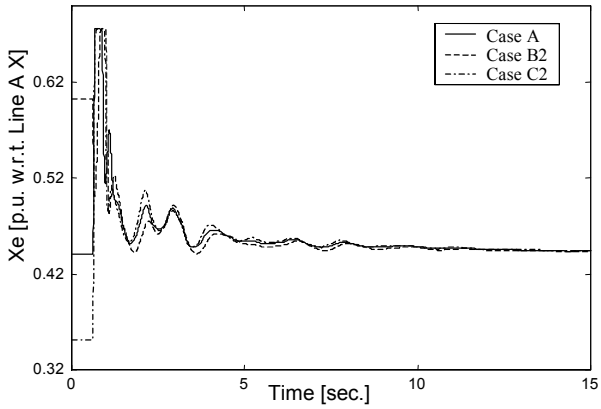

Fig. 19. TCSC equivalent reactance variations, variable post-contingency set point.

V. CONCLUSIONS

This paper provides a detailed analysis of some of the fundamental aspects of proper TCSC controller design. The limitations of using linear control techniques for controller design are discussed at length and illustrated in detail by studying the effect of large disturbances in a realistic power system network. A detailed analysis of TCSC control performance for improving system stability with different input signals is presented for a hierarchical TCSC control structure, illustrating the need for proper input signal selection and coordination of the different control levels. In particular, a study of the influence of set point values over controller performance is presented, proposing two different control strategies to avoid adverse interactions between the different hierarchical control loops of the TCSC.

VI. REFERENCES

[1] "Load Flow Control in High Voltage Power Systems Using FACTS Controllers," CIGRE Task Force 30.01.06, January 1996.

[2] "Thyristor Controlled Series Compensation," CIGRE Working Group 14.18, December 1997.

[3] C. Gama and R. Tenorio, "Improvements for Power System Performance: Modeling, Analysis and Benefits of TCSCs," Proc. IEEE/PES Winter Meeting, Singapore, January 2000.

[4] N. Martins, H. Pinto, and J. Paserba, "Using a TCSC for Power Scheduling and System Oscillation Damping–Small Signal and Transient Stability Studies," Proc. IEEE/PES Winter Meeting, Singapore, January 2000.

[5] "Impact of Interactions Among System Controllers," CIGRE Task Force 38.02.16, November 1999.

[6] G. Hingorani and L. Gyugyi, *Understanding FACTS: Concepts and Technology of Flexible AC Transmission Systems*, IEEE Press, 1999.

[7] A. Del Rosso, C. Cañizares, V. Quintana, and V. Doña, "Stability Improvements Using TCSC in Radial Power Systems," Proc. North American Power Symposium (NAPS), Waterloo, ON, October 2000. Available at www.power.uwaterloo.ca.

[8] J. Paserba, N. Miller, E. Larsen, and R. Piwko, "A Thyristor Controlled Series Compensation Model for Power System Stability Analysis," *IEEE Trans. Power Systems,* Vol. 10, No. 4, November 1995, pp. 1471-1478.

[9] C. A. Cañizares and Z. T. Faur, "Analysis of SVC and TCSC Controllers in Voltage Collapse ," *IEEE Trans. Power Systems*, Vol. 14, No. 1, February 1999, pp. 158-165.

[10] J. Machowski, S. Robak, and J. Bialek, "Damping of Power Swings by Optimal Control of Series Compensators," Proc. 10th International Conference on Power System Automation and Control, Bled, Slovenia, October 1997.

[11] N. Yang, Q. Liu, and J. McCalley, "TCSC Controller Design for Interarea Oscillations," *IEEE Trans. Power Systems*, Vol. 13, No. 4, November 1998, pp. 1304-1309.

[12] X. Chen, N. Pahalawaththa, U. Annakkage, and C. Kumbe, "Output Feedback TCSC Controllers to Improve Damping of Meshed Multi-Machine Power Systems," *IEE Proc. Trans. Distrib.*, Vol. 44, No. 3, May 1997, pp. 243-248.

[13] M. Noroozian, A. Wilk-Wilcznski, P. Halavarsson, and K. Niklasson, "Control Strategy for Damping of Power Swings Using TCSC," Proc. 6th Symposium of Specialists in Electric and Expansion Planning (VI SEPOPE), Brazil, 1998.

[14] P. Dolan, J. Smith, and W. Mittelstadt, "A Study of TCSC Optimal Damping Control Parameters for Different Operating Conditions," *IEEE Trans. Power Systems*, Vol. 10, No. 3, July 1995, pp. 1972-1978.

[15] "Power System Toolbox Ver. 2.0: Dynamic Tutorial and Functions," Cherry Tree Scientific Software, Colborne, ON, 1999.

Alberto D. Del Rosso received his Electromechanical Engineer diploma from the Universidad Tecnológica Nacional (UTN), Mendoza-Argentina, in March 1995, and his Ph.D. degrees in Electrical Engineering from the Instituto de Energía Eléctrica, Universidad Nacional de San Juan, San Juan, Argentina, in August 2001. Dr. Del Rosso was a Visiting Scholar at the University of Waterloo, E&CE Department, in the 1999-2000 academic year, and is currently working as a Power System Analyst at Mercados Energéticos, Buenos Aires, Argentina. His main areas of research interest are dynamic security and control of FACTS devices.

Claudio A. Cañizares received in April 1984 the Electrical Engineering diploma from the Escuela Politécnica Nacional (EPN), Quito-Equador, where he held different teaching and administrative positions from 1983 to 1993. His MS (1988) and PhD (1991) degrees in Electrical Engineering are from the University of Wisconsin-Madison. Dr. Cañizares is currently a Professor and Deputy Chair at the E&CE Department of the University of Waterloo, and his research activities concentrate mostly in studying stability, modeling, simulation, control, and computational issues in power systems.

Victor M. Doña obtained his Electrical Engineer diploma from the Universidad Nacional de San Juan (UNSJ), San Juan, Argentina, in March 1986. From 1986 to 1990 he worked for CONICET at the Instituto de Energía Eléctrica (IEE), UNSJ, San Juan, Argentina. From 1990 to 1993 he was a visiting researcher at the IAEW of the RWTH Aachen (University of Aachen), Germany. In 1993, he returned to work at the IEE and in 1996 received the Ph.D. degree in Electrical Engineering from the UNSJ. Dr. Doña is currently a Professor at UNSJ and his research and development activities include power system studies and software programming as a senior engineer, teaching and graduate supervision in the general area of security and optimization of power systems.